

INCORPORATION OF RIBONUCLEIC ACID BASES INTO THE METABOLIC POOL AND RNA OF *E. COLI*

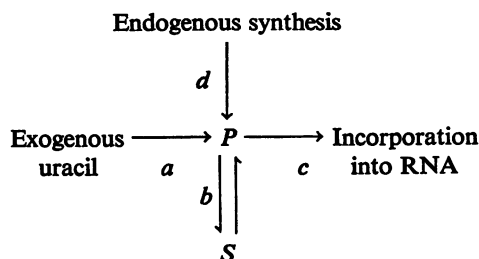
M. BUCHWALD *and* R. J. BRITTEN

From the Carnegie Institution of Washington, Department of Terrestrial Magnetism, Washington, D. C. Mr. Buchwald's present address is the Department of Biochemistry, Brandeis University, Waltham, Massachusetts

ABSTRACT Labeled cytosine, adenine, and guanine are rapidly incorporated by *E. coli*. A fraction of the radioactivity passes directly into RNA with very little delay. The remainder enters a pool before being incorporated into RNA. The fractions entering the pool and the time constants for equilibration of the specific activity of the pool are widely different for the four RNA bases.

INTRODUCTION

Studies of the incorporation of C¹⁴-uracil (McCarthy and Britten, 1962) showed direct entry of radioactivity into the ribonucleic acid (RNA) without delay by the large pool of nucleotides. The following schematic diagram was proposed to describe the kinetics of uracil incorporation.



P represents a very small pool or sequence of reaction steps leading from uracil to a chemical form suitable for incorporation into RNA. *S* represents a large pool of compounds which can exchange with some uracil compound in *P*. The rate of exchange between *S* and *P* is not fast, and equilibrium between the specific radioactivity of *P* and *S* requires several minutes, at least. Thus, according to this model, external uracil tracer may enter RNA without being delayed by passage through

the large pool (*S*). *P* then effectively forms a bypass around the large pool for the entry of exogenous uracil into RNA.

Since an alternative explanation of the undelayed entry of radioactivity into RNA has been proposed (Gros *et al.*, 1961) it seemed worthwhile to examine the kinetics of incorporation of the three other RNA bases. The additional information reported here clarifies the situation. The qualitative similarities and the quantitative differences in the kinetics of incorporation of the four RNA bases amply demonstrate the existence of direct pathways into RNA which bypass the large pools.

METHODS

All experiments were carried out with *E. coli* ML 30 growing exponentially in C medium (Roberts *et al.*, 1955) at 37°C with maltose as carbon and energy source. The generation time was 51 ± 2 minutes. The radioactive tracers used were cytosine-2-C¹⁴ (5.6 mc/mmole), guanine-2-C¹⁴ (6.5 mc/mmole), and adenine-8-C¹⁴ (10.0 mc/mmole) obtained from California Corporation for Biochemical Research, and Nichem, Inc.

Samples of whole cells or TCA precipitated cells were harvested on membrane filters (Britten *et al.*, 1955). The filters were air-dried at 60–70°C for half an hour and placed in a vial containing 10 ml of a 2, 5-diphenyl oxazole 4 gm/liter (PPO) and 1, 4-bis-2-(5-phenyl oxazolyl) benzene 100 mg/liter (POPOP) solution in toluene. The samples were counted in an automatic Packard Tri-Carb liquid scintillation counter. When it was desired to measure radioactivity remaining in the solution, the cells were removed by centrifugation and samples of the supernatant and resuspended pellet were counted with a thin window gas flow counter. Tests with uracil (McCarthy and Britten, 1962), guanine, and adenine show that, when the total incorporation curve ceases to rise, more than 95 per cent of the added radioactivity has been removed from the medium. In other words nucleic acid bases are not converted to non-utilizable compounds by *E. coli*. Chromatography also shows that greater than 85 per cent of the added radioactivity appears in the nucleotide residues of RNA.

The appearance of radioactivity in the four bases of RNA was determined in each case. For this purpose samples of the cells were treated with 5 per cent TCA, washed twice with water, and hydrolyzed in 0.380 N KOH overnight at 37°C. The KOH was absorbed on fine grain carboxylic ion exchange resin. The nucleotides were then separated by paper strip electrophoresis. The paper was dried and cut into strips which were counted in the liquid scintillation counter.

RESULTS

1. *Cytosine*. The results of an experiment in which 10^{-6} M cytosine-2-C¹⁴ was supplied to exponentially growing cells are shown in Fig. 1. It is clear that the kinetics of cytosine incorporation are qualitatively similar to the kinetics of uracil incorporation (McCarthy and Britten, 1962). There is an initial rapid incorporation into RNA, and this rate is maintained while exogenous cytosine remains. At the end of this first phase the rate of incorporation into RNA abruptly falls by a large factor. During the second phase (after the exogenous cytosine is exhausted) the radioactivity of the pool falls slowly. A semilog plot (Fig. 2) shows that the radio-

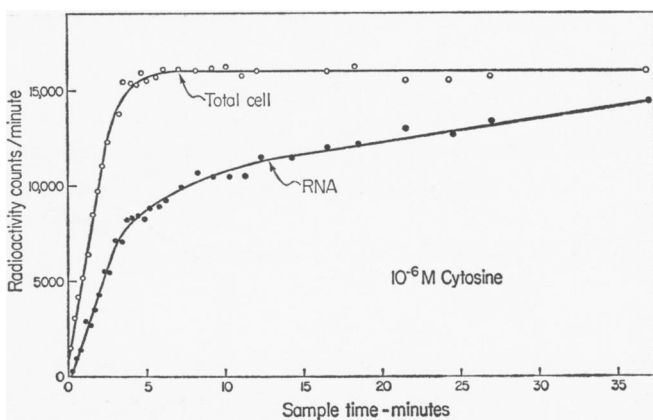


FIGURE 1 Incorporation of 10^{-6} M C^{14} -cytosine by *E. coli* ML 30 growing at 37°C with a generation time of 51 minutes. Cell density 0.5 mg (wet) per ml. Open circles represent radioactivity of total cell samples collected by membrane filtration. Solid circles represent RNA radioactivity; samples collected by membrane filtration after treatment with 5 per cent TCA.

Figs. 1 to 9 are reprinted from *Carnegie Institution of Washington, Yearbook No. 61, 1961-62*.

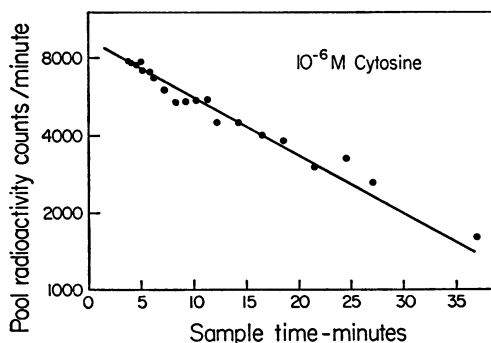


FIGURE 2 Decay of the radioactivity of the C^{14} -cytosine-labeled pool. Data obtained from experiment of Fig. 1 by subtracting the RNA radioactivity from the whole cell radioactivity.

activity of the pool decreases in an approximately exponential fashion. The time constant (decay to $1/e$) is about 21 minutes. This time constant is more than twice that observed for uracil. The results of an experiment at a higher concentration of cytosine (10^{-4} M) are shown on Fig. 3. Here again two phases are observed. Initially C^{14} from cytosine enters the RNA at less than half the final rate. Only after a relatively long period does it achieve its final rate.

The curves shown in Figs. 1, 2, and 3 are just those to be expected on the basis of the schematic diagram, if it is assumed that the time constant is a measure of the quantity of compounds in the pool (S) in relationship to the flow (b). The details of the procedure for the evaluation of the parameters of the model described by the schematic diagram are given in section 4.

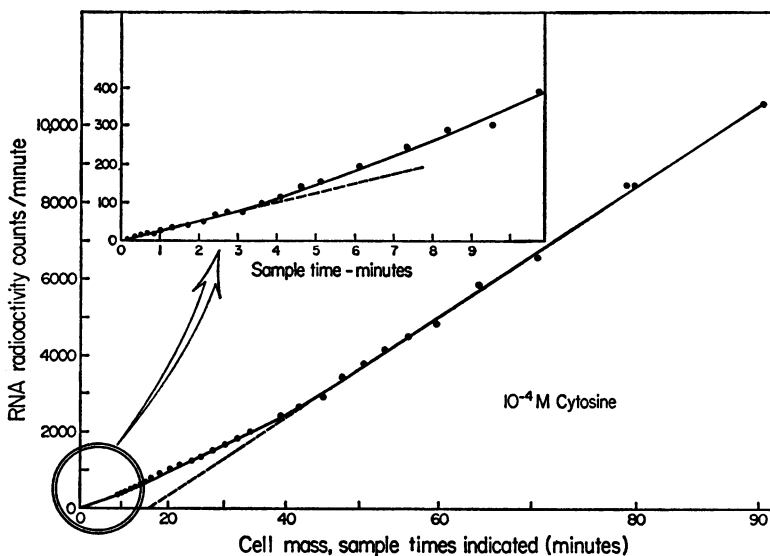


FIGURE 3 Incorporation of 10^{-4} M C^{14} -cytosine by *E. coli*. Initial cell density $\frac{1}{2}$ mg (wet) per ml. RNA radioactivity (TCA-precipitable) plotted against cell mass with sample times indicated. The upper curve represents the data at early times with both scales expanded by a factor of 10. Thus the slopes on the two curves may be directly compared.

The fraction of the total flow bypassing the pool (S) may be estimated from the fraction of the radioactivity (Fig. 1) that has entered the RNA at the time the exogenous cytosine is exhausted. This appears to be about 0.45 as shown in Table II, line 1. The bypass fraction of the flow may also be estimated from the ratio of the initial to ultimate slopes in Fig. 3. The result (Table II, line 2) is consistent with the results of the experiment at low concentration. The shape of the curve on Fig. 3 suggests the presence of components of intermediate time constant in the pool. However, their effect is not apparent on Fig. 2. If such additional components are present the time constant quoted is a weighted average, and the accuracy of the estimate of the bypass flow is reduced. The figure of 0.37 (Table II, row 2) is probably the better figure. Further discussion of the calculation of the bypass flow and time constants is given in section 4.

The time constant estimated here is probably influenced by the appearance of C^{14} from cytosine in uracil compounds in the pool and RNA. Table I shows the results of several measurements of the ratio of the amount of radioactivity in the uridylic acid to that in the cytidylic acid of the RNA. In view of the very considerable interconversion between cytosine and uracil compounds it is surprising that the effective time constants of pool (S) measured with the C^{14} -uracil and C^{14} -cytosine are so different. However, comparing lines 4 and 5 with lines 6 and 7 of Table I it appears

TABLE I
INTERCONVERSION OF CYTOSINE AND URACIL COMPOUNDS

Labeled supplement	Competitor	Ratio* of radioactivity of RNA uridylic to RNA cytidylic
C^{14} -cytosine $10^{-6}M$	—	1.4
C^{14} -cytosine $10^{-6}M$	—	1.6‡
C^{14} -cytosine $10^{-6}M$	—	1.7
C^{14} -cytosine $5 \times 10^{-6}M$	—	1.6
C^{14} -cytosine $5 \times 10^{-6}M$	C^{12} -uracil $5 \times 10^{-6}M$	0.6
C^{14} -uracil $5 \times 10^{-6}M$	—	1.0
C^{14} -uracil $5 \times 10^{-6}M$	C^{12} -cytosine $5 \times 10^{-6}M$	1.0

* After the radioactivity was completely incorporated into RNA the cells were washed with 5 per cent TCA, hydrolyzed with alkali, and the nucleotide residues separated by electrophoresis.

‡ In this experiment samples were taken at 10 minute intervals. By 10 minutes the ratio had already reached 1.3 and at 20 minutes had essentially reached its final value.

that C^{12} -uracil has an effect on the conversion of C^{14} -cytosine but C^{12} -cytosine does not affect the conversion of C^{14} -uracil. This lack of symmetry in the competition experiments and the relatively greater conversion of cytosine compounds to uracil compounds indicate the complexity of the interconversion processes.

2. *Guanine*. Fig. 4 shows the results of an experiment in which $10^{-6} M$ guanine was supplied to exponentially growing cells. Here again there is a rapid incorporation into RNA during the first phase when guanine is present externally. During the second phase after the external guanine has been exhausted the radio-

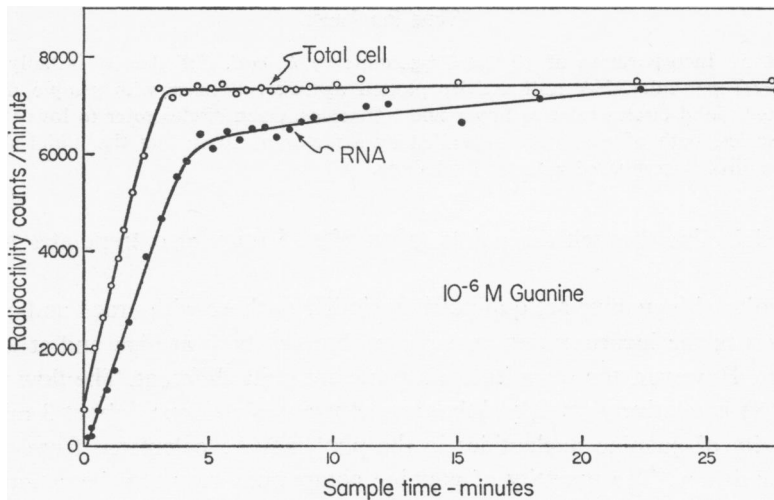


FIGURE 4 Incorporation of $10^{-6} M$ C^{14} -guanine by *E. coli*. Cell density 0.7 mg (wet) per ml. Open circles represent total cell radioactivity. Solid circles represent RNA radioactivity.

activity of the pool is relatively slowly transferred to RNA. No logarithmic plot of the decay of the guanine pool is presented since the relatively small amount of radioactivity in the pool and the scatter in the points lead to great inaccuracy. Various experiments have given mean time constants between 3 and 6 minutes for the decay of the pool radioactivity after the external guanine is exhausted.

Fig. 5 shows the results of an experiment in which a higher concentration of guanine (10^{-5} M) was supplied. Here a relatively small amount of curvature is observed

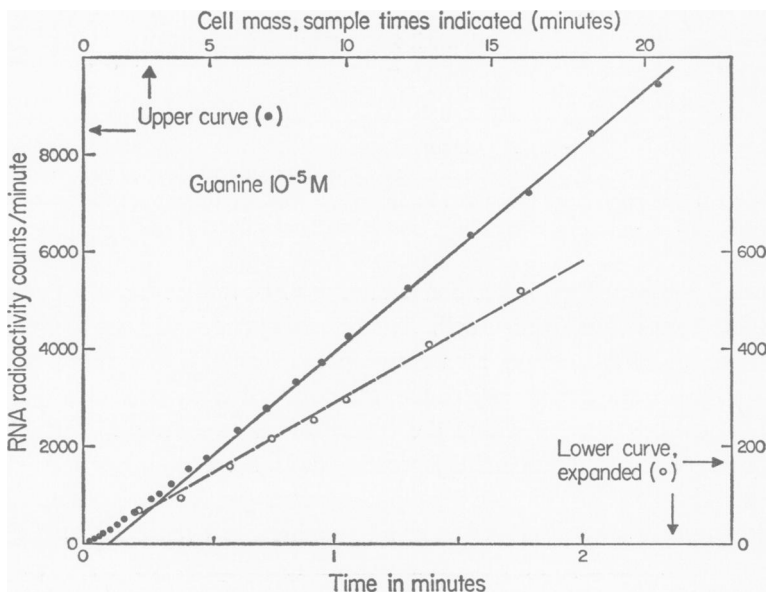


FIGURE 5 Incorporation of 10^{-5} M C^{14} -guanine by *E. coli*. Cell density initially 0.3 mg (wet) per ml. RNA radioactivity plotted against cell mass with sample times indicated. Solid circles refer to upper and left scales. Open circles refer to lower and right scales, both of which are expanded by a factor of 10 so that the initial slope may be directly compared with the final slope.

and a straight line through the points taken after 5 minutes extrapolates to about 1 minute.

The results with guanine are qualitatively similar to those with uracil and cytosine. Two phases in the incorporation curves are observed both at high and at low concentrations. However, the quantitative aspects are quite different. The flow through the pool (S) is relatively small and the time constant is not long (about 3 minutes). The quantity of guanine nucleotides in the pool may be calculated from the time constant and flow. The quantity of guanine compounds may also be estimated directly from the extrapolated time (Fig. 5) to be sufficient to supply the guanine required for 1 minute's growth of the cellular nucleic acid or 7μ moles per gram dry cells. This estimate is valid if there is little exchange between pool guanine compounds

and external guanine and if the conversion to adenine compounds is not too large. C^{14} -guanine does in fact appear only to a slight extent in the adenylic acid of RNA. In three experiments C^{14} -guanine at concentrations of 2×10^{-6} M, 10^{-5} M, and 5×10^{-5} M was allowed to be entirely incorporated into RNA. The ratio of the radioactivity of the adenylic acid of the RNA to that of the guanylic ranged between 0.1 and 0.2.

Fig. 6 shows the results of a "chase" experiment in which C^{14} -guanine ($3.6 \times$

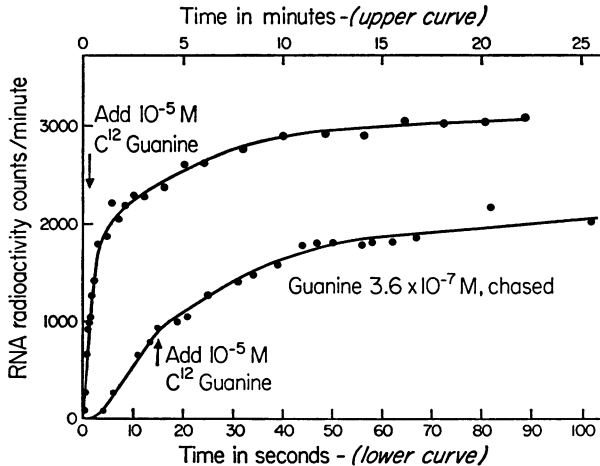
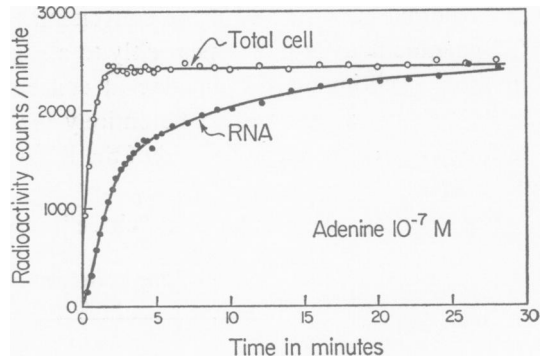


FIGURE 6 Guanine chase experiment. Exponentially growing *E. coli*, cell density 1.8 mg (wet) per ml. Initially C^{14} -guanine (3.6×10^{-7} M) was added. 15 seconds later C^{12} -guanine was added to bring the concentration to 10^{-5} M. Lower curve represents the same data as the upper curve but with time-scale (alone) expanded by a factor of 15.

10^{-7} M) was initially supplied to the cells followed 15 seconds later by 10^{-5} M C^{12} -guanine. This result differs from that obtained with uracil (McCarthy and Britten, 1962) where the specific activity of the uracil passing through the bypass appeared to be diluted almost instantly. In the case of guanine there appears to be a delay of 20 to 30 seconds before the tracer passing through the bypass is completely diluted. There is an instantaneous change in slope to about half that reached during the initial 15 seconds the undiluted tracer was present. This implies the existence in the pool of guanine compounds of a small component with a short time constant. Such a complexity is also suggested by the shape of the RNA curve on Fig. 4 just after the external guanine has been exhausted at 3 minutes, and by the uncertainty in the determination of the decay time constant for the pool of guanine compounds.

3. *Adenine.* Figs. 7 and 8 show the incorporation of C^{14} -adenine at 10^{-7} and 10^{-5} M. Here again the qualitative features are similar to those of the other three bases. Fig. 9 (derived from the experiment of Fig. 7) shows a semilogarithmic

FIGURE 7 Incorporation of 10^{-7} M C^{14} -adenine by growing *E. coli*. Cell concentration $\frac{1}{3}$ mg (wet) per ml. Open circles represent total cell radioactivity. Solid circles represent TCA-precipitable (RNA) radioactivity.



plot of the radioactivity of the pool after the external adenine was exhausted. It is immediately apparent that the decay of the pool radioactivity cannot be represented as a single exponential.

It might be proposed that the shape of the curve on Fig. 8 is influenced by a change in the pool size. The open circles represent the results of an experiment in which 10^{-5} M C^{12} -adenine was added 10 minutes before the tracer. There is no indication of any difference between the two curves on Fig. 8 other than that to be expected from the utilization of a certain fraction of the carrier adenine before the tracer was added. There was, therefore, no measurable expansion of the pool of adenine compounds even at this relatively high concentration of external adenine.

The appearance of radioactivity from C^{14} -adenine in the guanylic acid residues of RNA was measured at two concentrations (10^{-7} M and 10^{-5} M). In both cases the radioactivity of the adenylic residues was about three times that of the guanylic acid residues.

4. Calculation of the Bypass Flows and Time Constants. The schematic diagram given in the introduction describes a possible model which is consistent with the observations. The data presented in earlier sections permit the calculation of the parameters of this model. In this section procedures are described for the calculation of the bypass flow ($1-b/c$) and the time constant of the pool (S/b). These parameters have been calculated for each of the four bases from experiments at both high and low concentrations.

An experiment is considered to be at a low concentration if the external supply of labeled base is exhausted before the specific activity of the pool (S) has become comparable to the tracer specific activity. In other words the external supply is exhausted before the rate of incorporation of radioactivity has risen significantly above the initial rate.

If the external supply lasts well beyond the time when the final rate of incorporation into RNA has been achieved, little further change in the results occurs as the concentration is increased. Experiments at intermediate concentrations where neither of these conditions are met are more difficult to interpret.

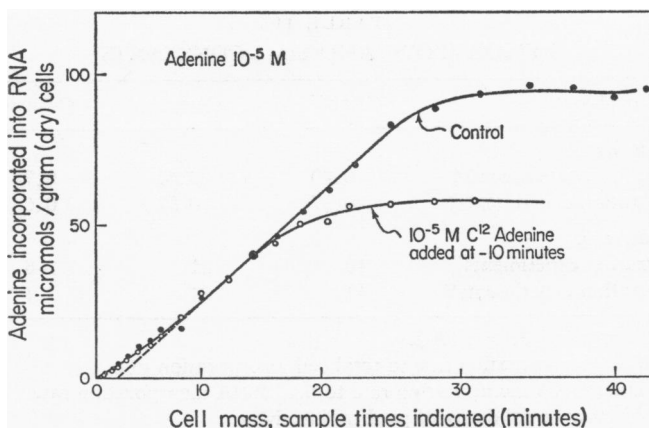


FIGURE 8 Incorporation of 10^{-5} M C^{14} -adenine by growing *E. coli*. Initial cell density 0.42 mg (wet) per ml. Solid circles, control. Open circles 10^{-5} M C^{12} -adenine added 10 minutes before carrier-free C^{14} -adenine.

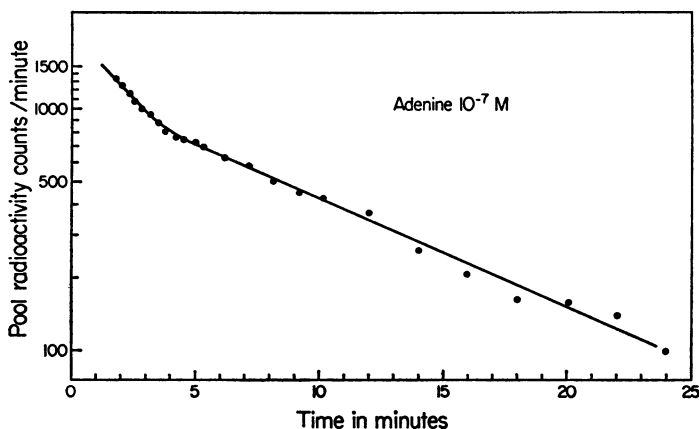


FIGURE 9 Semilogarithmic plot of radioactivity of pool after external adenine was exhausted. Data from Fig. 7.

For experiments at low concentration the bypass flow can be estimated directly from the fraction of the total radioactivity entering the cell that is fixed into the RNA. Thus $(c-b)/c$ listed in the first row in Table II was calculated from the ratio of the slopes of the RNA incorporation curve (TCA precipitable radioactivity) and the total curve. When experiments were available at both 10^{-6} and 10^{-7} M the results agreed.

For experiments at high concentrations the bypass flow was calculated from the ratio of the initial slope of the RNA incorporation curve to its slope after the final rate had been achieved (*i.e.* after S had reached its maximum specific radioactivity). Since there was significant cell growth, all the experiments at high concentration

TABLE II
BYPASS FLOWS AND TIME CONSTANTS

Base supplied	Uracil*	Cytosine	Guanine	Adenine
Fraction of flow in bypass				
Low concentration experiments‡	0.40	0.45	0.74	0.4
High concentration experiments§	0.37	0.37	0.68	0.46
Pool time constant, min.				
Low concentration experiments	10	21	2-6	2-12
High concentration experiments¶	11	24	3.1	4

* Data from McCarthy and Britten, 1962.

‡ From ratio of RNA incorporation rate to total cell incorporation rate.

§ From ratio of initial RNA incorporation rate to final RNA incorporation rate.

|| Time constant of exponential decay of pool radioactivity.

¶ Extrapolated delay time (corrected).

have been plotted against the increase in cell mass. Straight lines on such a plot correspond to constant rates of incorporation per cell. By marking the sample time on the abscissa it becomes possible to estimate directly the time constant by extrapolation (see below).

Row 3 (Table II) lists the time constant of the pool (S) estimated on semilogarithmic plots of the pool radioactivity as a function of time from experiments at low concentrations. The time constant estimated in this way is a measure of the ratio of the flow through the pool to the size of the pool if the pool is constant in size. There is no evidence that supplementation with RNA bases expands the nucleotide pools. In those cases that have been tested by "preload" experiments (adenine and uracil) certainly very little if any expansion occurs. The agreement between the data in row 3 and row 4 on Table II supports this conclusion.

Row 4 (Table II) lists the time constant for the increase in the rate of entry of radioactivity into RNA as it rises from its initial rate to its final rate. For this purpose the linear portion of the curve (*e.g.* Fig. 3) at late times is extrapolated until it strikes the time axis giving the effective delay time T' . To a sufficiently close approximation the desired time constant is given by $T = R_2 T' / (R_2 - R_1)$ where R_1 is the initial slope and R_2 the final slope.

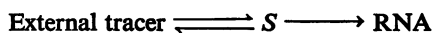
DISCUSSION

The evidence presented here and previously (McCarthy and Britten, 1962) shows that the incorporation of the four RNA bases may be represented by the schematic diagram given in the introduction to this paper. The relative bypass flow $(c-b)/c$, the size of the pool (S), and the time constant of the pool (proportional to S/b) vary widely among the four bases. The nucleotide pool appears to contain more than one component and the time course of the decay of the radioactivity of the pool is not always represented by a single exponential. Further, uracil compounds and cyto-

sine compounds are rapidly interconverted. Studies of cytosine (Table I) and uracil (McCarthy and Britten, 1962) show that some of this conversion occurs before entering the pool (S).

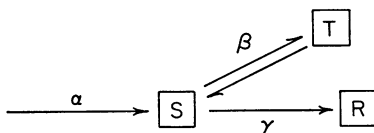
The schematic diagram would obviously grow in complexity if these features were explicitly indicated on it. It is clear that a very large number of significant steps have been ignored or briefly symbolized. As a result the question must be raised as to whether the central feature of the diagram—the existence of a bypass around the large pool—is indeed supported by the evidence.

In the first place it is clear that the evidence rules out models of the following type:



where the flow into RNA is just that required for growth. Such models are not consistent with an undelayed entry into RNA of a given fraction of the tracer that enters the cell (*e.g.*, Fig. 1) nor do they give any explanation of the second phase rise in rate observed in experiments at high concentration (*e.g.*, Fig. 3).

The only alternative that has been proposed (Gros *et al.*, 1961) which will explain the qualitative features may be represented by the following diagram, where S represents the nucleotide pool, R represents the stable RNA, and T represents an unstable (but TCA-precipitable) RNA. The flow γ is just that required for the growth of the stable RNA (R). The flow β is due to the turnover of the unstable RNA (T).



It has been proposed that RNA acting as template for protein synthesis might have the property of very rapid synthesis and breakdown (Jacob and Monod, 1961). If the flow (β) due to the turnover of T is very large, then T and S will effectively have the same specific radioactivity at any time. Thus a certain fraction (determined by the relative size of T and S) of the radioactivity entering the cell will appear without delay in TCA-precipitable RNA.

With the necessary assumption that the flow β is very large the previously presented data permit the calculation of both S and T for each of the four bases. The sum of S and T determines the time constants listed in Table II and the ratio $T/(T + S)$ gives the fraction of the tracer which enters the RNA without delay.

It is only necessary to compare the results for guanine with those for cytosine. When this calculation is carried out in detail it is found that this model requires the quantity of cytidylic acid in T to be 2.5 times the quantity of guanylic acid in T . However, the ratio of the guanylic acid to the cytidylic acid in the rapidly labeled RNA is 0.8 (Midgley and McCarthy, 1962).

Further, since all other RNA labeling will be delayed (according to this scheme) by the time constant determined by S plus T , the observed early labeled RNA must all be in the category represented by T . With uracil as tracer, the time constant of the early labeled RNA fraction is about $2\frac{1}{2}$ minutes (McCarthy *et al.*, 1962) and the time constant listed in Table II (from McCarthy and Britten, 1962) for S is 10 minutes.

Finally the early labeled RNA has been resolved into two distinct fractions (Bolton and McCarthy, 1962). About one-third hybridizes with DNA and appears to turn over by degradation with a time constant of $2\frac{1}{2}$ minutes. The remaining two-thirds does not hybridize with DNA to any large extent and has the same nucleotide composition as ribosomal RNA. There is little doubt that this fraction is precursor to ribosomal RNA and is not degraded before entry into the ribosomes. If this is so, the undelayed entry of tracer into this fraction must result from a bypass of the large nucleotide pools. Thus there is at present no reasonable alternative to the existence of a bypass around the nucleotide pools. It is not surprising that the nucleotide pools are bypassed for RNA synthesis, since the principal function of these pools may be other than in their role as nucleic acid precursors. ATP and other compounds act in the energy transport system, and it is likely that the pool compounds carry out other functions as well.

The relationship of the bypass to the mechanism of pool formation has been previously discussed (McCarthy and Britten, 1962). It was pointed out there that the carrier model (Britten and McClure, 1962) proposed for amino acid pools was consistent with the observations of uracil incorporation. Since the incorporation of the other three bases is in essential respects similar to that of uracil the carrier model gains further support.

Received for publication, July 31, 1962.

REFERENCES

- BOLTON, E. T., and MCCARTHY, B. J., *Proc. Nat. Acad. Sc.*, 1962, **48**, 1390.
BRITTEN, R. J., and MCCLURE, F. T., *Bact. Rev.*, 1962, **26**, 292.
BRITTEN, R. J., ROBERTS, R. B., and FRENCH, E. F., *Proc. Nat. Acad. Sc.*, 1955, **41**, 863.
GROS, F., GILBERT, W., HIATT, H., ATTARDI, G., SPAHR, P., and WATSON, J., *Cold Spring Harbor Symp. Quant. Biol.*, 1961, **26**, 111.
JACOB, F., and MONOD, J., *J. Molecular Biol.*, 1961, **3**, 318.
MCCARTHY, B. J., and BRITTEN, R. J., *Biophysic. J.*, 1962, **2**, 35.
MCCARTHY, B. J., BRITTEN, R. J., and ROBERTS, R. B., *Biophysic. J.*, 1962, **2**, 57.
MIDGLEY, J. E., and MCCARTHY, B. J., *Biochim. et Biophysica Acta*, 1962, **61**, 696.
ROBERTS, R. B., ABELSON, P. H., COWIE, D. B., BOLTON, E. T., and BRITTEN, R. J., *Carnegie Institution of Washington, Pub. No. 607*, 1955.